The Cryosphere Discuss., https://doi.org/10.5194/tc-2018-129
Manuscript under review for journal The Cryosphere
Discussion started: 11 July 2018

The Cryosphere Discussions
Open Access
EGU

Landfast sea ice stability – mapping pan-Arctic ice regimes with implications for ice use, subsea permafrost and marine habitats

Dyre O. Dammann[1], Leif E.B. Eriksson[1], Andrew R. Mahoney[2], Hajo Eicken[3], Franz J. Meyer[2]

[1]Department of Earth, Space, and Environment, Chalmers University of Technology, Gothenburg, 412 96, Sweden
[2]Geophysical institute, University of Alaska Fairbanks, Fairbanks, 99775, USA
[3]International Arctic Research Center, University of Alaska Fairbanks, Fairbanks, 99775, USA

Correspondence to: Dyre O. Dammann (dyre.dammann@chalmers.se)

Abstract. Arctic landfast sea ice has undergone substantial changes in recent decades affecting ice stability with potential impacts on ice travel by coastal populations and industry ice roads. The role of landfast ice as an important habitat has also evolved. We present a novel approach to evaluate sea ice stability on a pan-Arctic scale using Synthetic Aperture Radar Interferometry (InSAR). Using Sentinel-1 images from spring 2017, the approach discriminates between bottomfast, with critical relevance for subsea permafrost, as well as stabilized and non-stabilized floating landfast ice over the main marginal seas of the Arctic Ocean (Beaufort, Chukchi, East Siberian, Laptev and Kara Seas). The analysis draws on evaluation of small-scale lateral motion derived from relative changes in interferometric fringe patterns. This first comprehensive assessment of Arctic bottomfast sea ice extent revealed that by area most of the bottomfast sea ice is situated around river mouths and coastal shallows in the Laptev and East Siberian Seas, covering roughly 4.1 and 5.5 thousand km2 respectively. The fraction between non-stabilized and stabilized ice is lowest in the Beaufort at almost unity, and highest in the adjacent Chukchi Sea. Beyond the simple delineation of landfast ice zones, this work provides a new understanding of how stability regimes may vary between regions and over time. InSAR-derived stability data may serve as a strategic planning and tactical decision-support tool for different uses of coastal ice. Such information may also inform assessments of important sea ice habitats. In a case study, we examined an ice arch situated in Nares Strait demonstrating that interferograms may reveal early-warning signals for the break-up of stationary sea ice.

1 Introduction

1.1 Landfast sea ice stability and stakeholder dependence

Sea ice is an important component of Arctic ecosystems and provides important services as a climate regulator (Screen and Simmonds, 2010), habitat for marine biota (Thomas, 2017), as well as a platform for coastal populations (Krupnik et al., 2010). During the last century, an expansion of transportation and resource extraction have led to increased human presence in the Arctic and further diversification of ice use (Eicken et al., 2009). The recent retreat of sea ice observed throughout the past several decades (Stroeve et al., 2012;Comiso and Hall, 2014;Meier et al., 2014) has already resulted in widespread consequences for ice users (Druckenmiller et al., 2013;Aporta and Higgs, 2005;Fienup-Riordan and Rearden, 2010;Orviku et al., 2011;ACIA, 2004) and increasing hazards (Eicken and Mahoney, 2015;Ford et al., 2008). At the same time, the related increased accessibility to Arctic waters (Stephenson et al., 2011) is leading to increasing ship traffic and resource exploration (Lovecraft and Eicken, 2011;Eguíluz et al., 2016). It is recognized that the sea ice conditions for future Arctic marine operations will be challenging and will require substantial monitoring and improved regional observations (Ellis and Brigham, 2009) at the scale necessary for assessing environmental hazards and effective emergency response (Eicken et al., 2011).

The Cryosphere Discuss., https://doi.org/10.5194/tc-2018-129
Manuscript under review for journal The Cryosphere
Discussion started: 11 July 2018

Most of the Arctic ocean is dominated by drifting pack ice, whereas stationary landfast ice occupies much of the Arctic coastlines roughly between November and June depending on location (Figure 1) (Yu et al., 2014). Although the landfast ice is stationary, it does deform internally at the cm- to m-scale on timescales of days to months (Dammann et al., 2016). The often several km to up to hundreds of km wide sections of landfast ice are held in place by grounded ridges, islands, or coastline morphology, such as embayments or fjords. Similar to the drifting pack ice, landfast ice has declined significantly during the last few decades, in particular in terms of delayed freeze up (Mahoney et al., 2014;Selyuzhenok et al., 2015) critically impacting stakeholders through reduced stability, defined here as the immobility (at spatial dislocation scales of meters or more) of the landfast ice in response to wind, ocean, or ice forcing (Dammann, 2017). Previous research suggests that landfast ice stability can be expressed in terms of the combined frictional resistance provided by relevant grounding or attachment points (e.g., islands and grounded ridges) (Druckenmiller, 2011;Mahoney et al., 2007b), which in part determines the rate at which the ice deforms and ultimately the severity of break-out events or magnitude of structural defects. We therefore suggest that landfast sea ice can be further categorized into four regimes, defined through their respective stability (Table 1). A typical landfast ice regime is illustrated in Figure 2, where the stability of the landfast ice area decreases from left to right (Dammann et al., 2016).

Bottomfast sea ice can grow to the km-scale during winter depending on local bathymetry (Solomon et al., 2008;Stevens et al., 2010). The bottomfast ice allows for heat loss from the sea floor and is therefore an integral part of aggregating and maintaining subsea permafrost (Stevens et al., 2008;Stevens et al., 2010;Stevens, 2011), controlling coastal stability/morphology (Eicken et al., 2005;Are and Reimnitz, 2000), and sediment properties (Solomon et al., 2008). Bottomfast ice is also relevant for fish as it reduces habitable shallow waters during winter (Hirose et al., 2008). Bottomfast ice is also of importance for on-ice operations as it can support a much larger load than floating ice. High to moderately stable landfast is of relevance to industrial (Potter et al., 1981) and subsistence ice use (Druckenmiller et al., 2013), but also for habitats. For instance, ringed seals are dependent on stable landfast ice for denning (Smith, 1980). Low-stability ice is potentially relevant for ocean-based operations such as trans-Arctic and destinational cargo shipping as it provides opportunities for docking in areas of substantial landfast ice and when making passages close to the coast where landfast ice is present. Here, particularly grounded ridges are problematic and associated with hazards (Hui et al., 2017). In addition, patches of landfast ice occasionally break off and drift into nearby shipping lanes, potentially causing hazards. Ice arches (Kwok et al., 2010), which are forming between islands during freeze-up, are another form of stationary ice of high relevance for navigation. When they potentially collapse in the spring, hazardous old ice can get exported into shipping routes (Bailey, 1957;Wilson et al., 2004;Barber et al., 2018).

1.2 Remote sensing of landfast sea ice stability

Satellite remote sensing is an important tool for measuring ice conditions in the Arctic due to spatially sparse in-situ data, including delineation of landfast ice (Muckenhuber and Sandven, 2017). Optical/thermal satellite data such as from the Advanced Very High Resolution Radiometer (AVHRR) were used to produce operational ice charts until the early 1990s when SAR was introduced into the charting production (Yu et al., 2014) as a superior data set due its independence of light and weather conditions and due to its higher (~100 m) resolution, both advantageous to stakeholders (Eicken et al., 2011). Different information products exist to delineate the boundary of landfast sea ice, typically derived by evaluating unchanged sections of ice between consecutive SAR backscatter scenes either visually (Johannessen et al., 2006), based on spatial backscatter gradients (Mahoney et al., 2014), or based on boxcar image cross correlation (Giles et al., 2008). Beside its use in delineation of landfast ice, SAR backscatter also has the ability to help identify different ice types and roughness regimes (Dammann et al., 2017), but does not give information pertaining to the stability of the ice.

The Cryosphere Discuss., https://doi.org/10.5194/tc-2018-129
Manuscript under review for journal The Cryosphere
Discussion started: 11 July 2018

SAR interferometry (InSAR) is a signal processing technique, which extracts the phase difference between SAR images acquired from similar viewing geometries. This phase difference (typically referred to as interferometric phase) can either signify sea ice topography if acquisitions are separated in space (i.e., non-zero perpendicular baseline) or measures the line-of-sight motion of an observed feature if acquisitions are separated in time (non-zero temporal baseline). InSAR has been used to successfully delineate landfast ice (Meyer et al., 2011) as well as to provide information pertaining to landfast ice dynamics (Marbouti et al., 2017;Li et al., 1996;Vincent et al., 2004;Morris et al., 1999) and topography (Dammann et al., 2017;Dierking et al., 2017). In recent studies, InSAR has also been shown to reveal plausible rheologies for landfast ice (Dammert et al., 1998) and has been used to determine the origin of internal ice stresses (Berg et al., 2015). Combined with inverse modeling, InSAR also allows to determine ice deformation modes (Dammann et al., 2016), rates, and the associated stress and fracture potentials (Dammann et al., 2018b).

The studies cited in the previous section here have demonstrated the potential of InSAR as a tool to assess landfast ice dynamics and stability through localized case studies. They also laid the foundation for applying InSAR on a larger scale, potentially as a means to generate operational information products and evaluate long-term trends. The coverage and access to InSAR-compatible SAR scenes has been an obstacle in the past, but has improved significantly since the launch of Sentinel-1. The suitability of Sentinel-1 for automatic SAR processing was shown, e.g., in Meyer et al. (2015). Hence, we explore InSAR as a tool to provide pan-Arctic information relevant to monitoring of subsea permafrost, biological habitats and sea ice use by providing information pertaining to landfast sea ice stability. The goal of this work is to determine the ability to create interferograms of the different ice regimes outlined in Table 1 (*Section 3.1*), and further analyze interferograms along substantial parts of the circumpolar coastlines to assess the performance and coverage of InSAR data across different geographic regions (*Section 3.2*). We further explore limitations of the technology and the utility for long-term assessments of change. We also evaluate the kind of sea ice information that can be extracted directly from InSAR with operational relevance in terms of tactical and strategic decision making, without costly or complex algorithms (*Section 4*).

2 Data and methods

2.1 Satellite data and study area

This study utilizes Sentinel-1, a constellation of two C-band SAR systems (Sentinel-1A and B) operating since 2014 and 2016, respectively, with a repeat-pass interval of 6 to 12 days depending on if both satellites acquire data or only one of them. The resolution is 5m x 20 m in single look, which we reduced to 50 m x 40 m through multilooking. Owing to the free-and-open data policy and large spatial coverage (~250 km swath width for interferometric wideswath (IW) mode data), Sentinel-1 acquisitions were obtained for five marginal seas of the Arctic ocean including the Beaufort, Chukchi, East Siberian, Laptev, and Kara Seas during the months of March through May 2017, enabling mapping of landfast sea ice on a pan-Arctic scale. Of these regions, the Beaufort Sea coast of Alaska was used for validation, as the sea ice in this area includes all four landfast ice regimes (bottomfast ice, semi-enclosed lagoon ice, ice stabilized by grounded ridges and islands, and areas with floating extensions of ice; Table 1), and as ample validation data is available from previous landfast sea ice studies. Alaska's Beaufort Sea coast is also of major interest in the context of local and indigenous ice use as well as industry resource exploration and extraction.

2.2 InSAR-based detection of landfast ice

InSAR is a technique that measures the phase difference between two complex SAR scenes obtained from similar viewing geometries (Ferretti et al., 2007;Bamler and Hartl, 1998). The phase change may be related to the lateral (e.g., thermal

contraction or displacement due to compressional or shear forces) or vertical sea ice motion (e.g., through buckling or tidal displacement) occurring in between the acquisition times of the two InSAR images. Depending on the perpendicular baseline, sea ice topography can have a modest impact on the phase difference. Due to the tight baseline limits of the Sentinel-1 constellation and as sea ice topography rarely exceeds 10 m, impacts on the interferogram interpretation are minimal for the data shown here (Dammann et al., 2016). Only displacement in line-of-sight direction (Δr_{LOS}) results in a phase change $\Delta\Phi_{disp}$ according to $\Delta\Phi_{disp} = 4\pi\,\Delta r_{LOS}/\lambda$ and the observed phase is measured within the wrapped interval of $[0; 2\pi]$. For Sentinel-1, the sensor wavelength λ is 5.66 cm, such that ice displacement has to exceed $\Delta r_{LOS} \approx 5cm$ for the $\Delta\Phi_{disp}$ phase values to "wrap around". The result is a series of fringes representing the projection of the true three-dimensional ice motion onto the line-of-sight vector. The orientation of the fringes can be used to interpret the direction of the three-dimensional motion field while the fringe spacing is an indicator of the deformation rate. The interpretation of observed fringe patterns is, however, not straightforward typically requiring the use of an inverse model (Dammann et al., 2016). An interferogram can only be successfully created if scattering elements remain largely unchanged throughout the time interval bracketed by the image pairs used in processing. Coherence (ranging between 1 and 0) is a measure of the quality of the interferogram, which in general is high if scatterers remain unchanged and low if there is significant change in the scattering medium. A complete list of potential sources of decorrelation are described in (Meyer et al., 2011). For the 6 or 12 day repeat cycle supported by Sentinel-1, the coherence over landfast ice was found to be generally high due to its stationary nature. Significant decorrelation can however occur in late spring as the onset of melt at that time causes substantial changes in the scattering medium. In this work, we have obtained images as close to late April as possible. This time frame was found to be ideal for our purpose as ice thickness is near its maximum leading to maximum stability without risking impacts from the onset of melt. All interferograms in this work were produced using a standard Sentinel-1 workflow including multi-looking, coregistration, interferogram formation, and geocoding using the GAMMA RS software (Werner et al., 2000).

2.3 Pan-Arctic delineation of landfast ice regimes

In this work, we are looking at the fringe spacing to roughly determine relative strain rates as an indicator of stability with a lower density corresponding to higher ice stability. There are many factors that affect fringe density, including the satellite viewing geometry and the prevalent mode of ice deformation (Dammann et al., 2016). Hence, we focus on abrupt variations in fringe spacing that allow us to identify the zones outlined in Table 2. As compared to Table 1, the two sheltered regimes have been merged to "stabilized ice" since they are potentially difficult to discriminate strictly based on InSAR data. These three regimes are subjectively and manually delineated without the use of specific threshold values. The regimes themselves are therefore based on relative stability in terms of whether the ice is anchored or sheltered. A measure of whether the ice is stable would depend on the specific stakeholders and their dependence on stability. As an example, on shorter time scales, industry ice roads would be able to accommodate less strain than community ice trails due to different mode of transportation and user specific needs. Further steps to identify such thresholds are outlined in Dammann et al. (2018a).

The approach taken in this study opens up the possibility of delineating landfast sea ice regimes on a pan-Arctic scale. To demonstrate, we used Sentinel-1 data acquired March through May 2017 and generated 50 interferograms that cover almost the entire continental coastlines of the Beaufort, Chukchi, East Siberian, Laptev, and Kara Seas. To reduce computational costs, we omitted Greenland, some island groups and in particular the Canadian Archipelago, which are characterized by extensive coastline lengths. We also emphasized the Alaskan and Russian coastlines due to their high economic significance for the shipping and natural resource industries and due to the diverse ice stability regimes and larger areas of bottomfast ice expected in these regions. Except for one approximately 50 km-long section of coast in the Kara Sea, multiple InSAR compatible pairs were

available for the specified time frame, allowing us to select interferograms centered around the end of April, when most Arctic landfast ice is at its maximum extent. Coherence loss was evident in some areas, in particular in the Chukchi Sea, such as in the Kotzebue Sound likely partly due to ice motion, subsurface thinning from river runoff, and low signal-to-noise ratio. However, to ensure a realistic representation of what an operationally-produced synoptic, contiguous pan-Arctic interferogram would look like, we did not attempt to derive alternative interferograms in these cases.

3 Results

3.1 Validating InSAR-derived ice regimes in the Beaufort Sea

We explored the utility of InSAR to aid in delineation of different landfast ice regimes across the majority of the Alaska Beaufort Sea coastline. Here, the landfast sea ice has been extensively researched and tracked in terms of its annual cycle and decadal variability (Mahoney et al., 2007a;Mahoney et al., 2004). The resulting stack of all landfast ice edge delineations derived from three consecutive SAR images for all months between 1996 and 2008 (Mahoney et al., 2014) is plotted in Figure 3a. From this figure, it is clear that in certain regions, the ice extent is similar over time scales from months to years (see areas highlighted in the figure). It was found that these regions of consistent landfast ice extent are often tied to the location of the 20-m isobath, a waterdepth associated with grounding of pressure ridges (Mahoney et al., 2014). Key locations of such landfast ice edge "nodes" are marked on the figure as a-c. A field study and Indigenous knowledge indicate that node "a" corresponds to an area of persistent grounded ridges that stabilize the sea ice near Utqiaġvik, Alaska (Meyer et al., 2011).

We created three interferograms acquired during the period April 8 – May 9 to cover the same stretch of coastline (Figure 3b). These interferograms reveal a wide range of fringe densities, ranging from near constant phase for areas close to the coast to the point where fringes are dense enough to almost merge near the landfast ice edge. It is also apparent that the fringe density does not linearly increase with distance from the coast, but rather changes along two distinct discontinuities. One discontinuity separates the area of near-zero phase change from an area with relatively low fringe density (i.e., no consistent fringe pattern visible). This gradient has been shown to delineate the boundary between bottomfast and floating sea ice (Dammann et al., 2018c).

The second discontinuity appears to largely coincide with locations of the nodes identified by Mahoney et al. [2007a; 2014], which are thought to be associated with recurring grounded ice features (Figure 3a) (Meyer et al., 2011). This finding is expected since grounded ridges are known to stabilize the landfast ice leading to reduced strain shoreward of the grounding points (Mahoney et al., 2007b;Druckenmiller, 2011), resulting in reduced phase response. The discontinuity is not a straight line, but features multiple seaward points of higher stability consistent with the expected increased stability directly adjacent to grounded ridges. We performed a subjective, manual delineation (i.e. without the use of a specific threshold) of the strong phase gradients in Figure 3c and concluded that the ice regions separated by these discontinuities consist of non-stabilized, stabilized, and bottomfast ice (Figure 3d).

3.2 Deriving pan-Arctic landfast sea ice stability regimes

The interferograms produced in this work (Figure 4) allowed for a detailed delineation of landfast ice including the identification of three landfast ice stability regimes: bottomfast ice, stabilized landfast ice, and non-stabilized landfast ice (see *Section 2.3*). To our knowledge, our results (Figure 5) represent the first mapping of bottomfast ice extent at this scale and the first attempt at any scale to map the extents of different landfast ice stability regimes. Subject to the considerations discussed in *Section 4.1,* it is

clear that most areas with substantial bottomfast ice are located either in the vicinity of river deltas or within lagoons. However, a prominent exception is the coastline of the western East Siberian Sea, where our analysis shows substantial amounts of bottomfast ice even tens of kilometers away from any major rivers. Accordingly, the East Siberian Sea with its three large river systems (the Indigirka, Bogdashkina, and Kolyma Rivers) contains the most bottomfast ice of the regions considered here (Table 3). The Laptev Sea also contains a large fraction of the Arctic bottomfast sea ice mostly concentrated around the Lena and Yana Deltas.

The delineation of "stabilized" and "non-stabilized" landfast ice in Figure 5 is based on subjective interpretation of the interferograms shown in Figure 4 using the criteria described in *Section 2.3*. Both stabilized and non-stabilized landfast ice regimes were found in all marginal seas (Table 3), though their relative contributions to overall landfast ice extent varied widely. For example, in the Chukchi Sea, we identified the vast majority of the landfast ice as non-stabilized, with stabilized landfast ice occupying only slightly more area than bottomfast ice. Conversely, the greatest area of stabilized landfast ice was found in the adjacent Beaufort Sea, where non-stabilized landfast ice contributed an approximately equal amount to the overall extent of landfast ice.

In the East Siberian, Laptev and Kara Seas, the distinction between stabilized and non-stabilized landfast is not as straightforward as in the Beaufort and Chukchi Seas. We speculate that this may be caused by a lower level of pack ice interaction along the Russian shelf, given the predominantly divergent ice regime (Reimnitz et al., 1994;Jones et al., 2016;Alexandrov et al., 2000), leading to reduced dynamically-induced strain (and therefore fewer interferometric fringes) in landfast ice seaward of offshore islands and grounded ridges. Additionally, the greater extent of landfast ice on the shoreward side of grounding points provides a greater fetch, which may cause stabilized ice on the Russian Shelf to exhibit higher fringe densities than in the Chukchi or Beaufort Seas. Despite these caveats, it is clear that landfast ice extent in the East Siberian, Laptev and Kara Seas is dominated by vast areas of non-stabilized ice. However, unlike the Chukchi Sea, we still identified significant areas of stabilized landfast ice. In the Kara Sea, these are primarily found between the islands of the Nordenskiöld Archipelago in the east, but the most extensive regions of stabilized landfast ice in our study region (those that extend furthest from the coast) are found in the Laptev and East Siberian Seas (areas labeled A, B, and C in Figure 5). Another important region of stable landfast ice is the New Siberian Islands, but was not considered here as outlined in *Section 2.3*.

4 Discussion

4.1 Methodological limitations for different stability classes

Although there are a number of sources of uncertainty that affect our delineation of landfast ice and its relative stability, it is clear that not all landfast ice is equally stable and at least three different classes of stability can typically be identified. In some areas, the delineation of bottomfast ice has had to be approximated on the sub-km-scale due to ambiguities associated with low fringe density or fringes parallel to the bottomfast ice edge (Dammann et al., 2018c). We also acknowledge that small islands or sandbars not represented by our coast mask may be erroneously identified as bottomfast ice. However, we feel these uncertainties are unlikely to significantly affect our findings at regional and pan-Arctic scales. The sources of uncertainty affecting the distinction between stabilized and non-stabilized landfast ice are more numerous and warrant greater discussion.

In this work, we did not apply strict delineation thresholds to distinguish between stabilized and non-stabilized ice, but rather made subjective determinations based on fringe patterns. This approach works well in the Chukchi and Beaufort Seas, where regions of low fringe density lie adjacent to the coast or bottomfast ice and can be easily delineated from regions of higher fringe

density. However, in some regions, especially in the Russian Arctic, there is often a lack of distinct boundaries between regions of different fringe spacing, introducing ambiguities between stabilized and non-stabilized ice on scales from km to even tens of km. As discussed in *Section 3.2*, the difficulty distinguishing these two classes of landfast ice in the Russian Arctic may result from a reduced level of dynamic pack ice interaction (making the non-stabilized ice appear more stable) and a larger fetch of ice shoreward of pinning points (making the stabilized ice more susceptible to wind and tidal stresses). This suggests, that there is likely a spectrum of landfast ice stability and additional classes may be necessary to fully characterize the landfast ice regimes in different regions and for different ice uses or research aims.

One potential candidate for reclassification is landfast ice in sheltered bays such as the Khatanga Gulf in the western Laptev Sea, which exhibited high fringe densities (Figure 4) and was hence identified as non-stabilized despite being nearly landlocked (Figure 5). Due to the shallow water in this region, it is likely that the high fringe density is caused in part by vertical motion associated with tides and coastal set up. Since vertical motion has less impact on stability in well-confined landfast ice, such examples suggest the need for an additional class of stability that allows higher fringe densities in coastally confined regions. Another, larger-scale example is the eastern Laptev sea, which is an area of landfast ice sheltered by the New Siberian Islands and is typically considered highly stable (Eicken et al., 2005). However, based on relatively high fringe density, in particularly offshore of the Lena Delta, we classify landfast ice in this region as non-stabilized (Figure 5). This suggests that landfast ice in this region may be less stable than previously thought and a "partially stabilized" class may be appropriate. This would be consistent with a recent SAR-based analysis of landfast ice in the Laptev Sea (Selyuzhenok et al., 2017), which showed that areas identified as landfast ice in operational ice charts may actually contain pockets of partly mobile ice over one month after initial landfast ice formation.

The number of useful classes of landfast ice stability is limited by other inherent sources of uncertainty including sensitivity to specific atmospheric and oceanographic conditions during the time period between SAR acquisitions. For example, in the absence of dynamic interaction with pack ice, there may be little difference in fringe spacing between landfast ice seaward and shoreward of stabilizing anchor points. Without evaluating the phase response for each area of interest in detail during different forcing scenarios, it may be problematic to understand under what conditions the ice remains stable. Classification of stability based on relative differences in fringe density is also complicated by the use of non-simultaneous interferograms to provide complete coverage of a region. The interferograms used here were obtained as close to maximum ice extent and stability as possible (roughly late April), but sometimes had to be obtained as early as early March. As discussed below in *Section 4.2*, fringe density tends to decrease over the winter as the ice thickens. Hence, the use of interferograms based on different dates can result in a phase gradient at the image stitching not related to different stability regimes, which may further complicate the delineation process (e.g. northernmost region of the Lena Delta featured in Figure 4).

The Sentinel-1 interferograms considered here has a minimum temporal baseline of 12 days. Even if this baseline is shorter than what has been used in the past (Dammann et al., 2016;Mahoney et al., 2004), it is unlikely that the delineation of the seaward landfast ice edge incorporates stationary pack ice (as could possibly be the case for a 6-day baseline). The availability of Sentinel-1 IW data decreases away from the coast and so it may not be possible to obtain imagery over the seaward most areas of extensive landfast ice approaching the 250 km IW swath such as that in the East Siberian and Laptev Seas. Also, some regions feature consistent coherence loss such as the Kotzebue Sound region. Such regions can most often be identified through a gradual progression from high coherence to a complete loss of coherence, where an exact delineation of landfast ice type boundaries is not possible. Furthermore, this technique can only be used before the onset of melt when widespread coherence loss occurs.

The Cryosphere Discuss., https://doi.org/10.5194/tc-2018-129
Manuscript under review for journal The Cryosphere
Discussion started: 11 July 2018

4.2 Temporarily stabilized pack ice

Prior studies have demonstrated the utility of InSAR over landfast ice as a planning tool for on-ice operations (Dammann et al., 2018a;Dammann et al., 2018b) but we argue here that such utility and potential applications also extend to maritime activities and shipping. In regards to the latter, vessel traffic typically does not traverse landfast ice. However, the assessment of landfast ice stability and spatio-temporal extent can aid management of conflicting ice uses such as in the case of the access route to the Voisey's Bay mine in the Canadian Arctic which cuts through landfast ice that is part of a traditional Nunatsiavummiut use area (Bell et al., 2014). For vessel traffic through ice-covered straits or archipelagos, the approach outlined here can help identify and evaluate hazards associated with ice arches. Ice arches form when ice passing through a narrow passage experiences flow stoppage as a result of confining pressure and behaves like landfast ice, though potentially without cohesive strength between individual floes (Hibler et al., 2006). Indeed, ice arches may be considered as an additional class of "temporarily stabilized pack ice". When formed, such arches represent a significant obstacle to marine traffic due to the high confining pressures that make icebreaking impossible for all but the most powerful vessels. Conversely, their break-up can lead to advection of large amounts of thick multiyear into high-traffic shipping routes (Barber et al., 2018).

A commonly occurring ice arch is situated in Nares Strait in between Greenland and Ellesmere Island (Kwok et al., 2010). In 2017, Sentinel-1 SAR imagery captured the formation and break-up of this arch. The arch was relatively stable on 6 May (Figure 6a) before eventually failing sometime before 12 May (Figure 6b). Here the line of failure is identified in Figure 6b and marked in both panels. A sequence of six interferograms (Figure 7) with a 6-day temporal baseline covering a timespan of 36 days indicates ice deformation around the failure line up until the failure event. The ice arch features various levels of cm- to m-scale deformation and fractures resulting in fringe discontinuities (Figure 7a) most pronounced near the arch terminus to the south. Near the failure line, there is no sign of a fringe discontinuity up until 12 April (Figure 7a) when the interferogram displays near cross-track parallel fringes indicating compression towards the terminus (Figure 7b). There is a significant contrast in fringe density on either side of the line which may be indicative of a fracture where ice to the west is being compressed more rapidly than the ice close to the coast. The interferogram between 18 – 24 April features widespread coherence loss possibly due to continued compression (Figure 7c). Deformation is less severe from 24 April when fringe density is significantly reduced. However, we notice a fringe discontinuity to the east of the line featuring perpendicular intermediate fringe patterns towards late April (Figure 7d). These patterns develop further into circular patterns often associated with vertical lifts and depressions (Figure 7e) before the whole arch appears to fail through shear motion along this same fault (Figure 7f).

This example demonstrates that it may be possible to detect precursors to break-out events without rigorous inverse model-based interpretation of fringe patterns (e.g., Dammann et al., 2016;Dammann et al., 2018b), which does not easily lend itself to operational workflows. Evaluating the interferograms leading up to the failure of the ice arch, suggests that InSAR has the ability to inform stakeholders of changing stability and ice movement with potential value for an early warning system designed to alert ice users of hazards related to ice movement. Recent and ongoing sea ice decline is leading to an increasing presence of dynamic ice, which may result in earlier breaching of ice arches. This may in turn result in a larger quantity of advected ice with potentially longer travel paths increasing the severity of such events (Barber et al., 2018).

4.3 InSAR as a monitoring tool for landfast ice stability

The method presented in this work has a broad set of applications for monitoring including subsea permafrost, biological habitats both beneath and above the ice surface, and ice use by a range of stakeholders. Bottomfast ice is important because it helps aggregating subsea permafrost constraining the location of permafrost-rich shorelines. Utilizing InSAR, it is likely possible to

monitor changes in bottomfast ice over time with significant implications for erosion and spring flooding (Dammann et al., 2018c) and the release of methane hydrates (Brothers et al., 2012). With respect to ice users, sea ice navigation near or through landfast sea ice is presently predominately supported by sea ice charts that delineate areas occupied by landfast ice, but do not provide information as to the relative stability of the ice. The information provided here would likely be useful in the context of navigation and supporting on-ice operations and could be provided through the InSAR-based approach described here by identifying the following stability-related features:

1) Low-stability ice that may break off and drift into shipping lanes.
2) Grounded ridges that may be problematic for ice navigation, but at the same time may provide added stability for on-ice operations.
3) Stable areas to use for equipment staging by coastal community hunters and industry.
4) Bottomfast ice for development of ice roads for transportation of heavy loads.

In this work, no parameters were changed in the interferometric processing workflow between regions or image pairs emphasizing the possibility of producing these images in a cost-effective manner and by personnel with limited experience with InSAR, similar to semi-automated processing underlying SARVIEWS (http://sarviews-hazards.alaska.edu) and HyP3 (http://hyp3.asf.alaska.edu). The method of delineating landfast ice stability is further based on visual interpretation. We have based the analysis strictly on identifying areas of reduced phase response or a strong phase gradient without applying other datasets or advanced interpretation methods such as inverse modeling. Hence, the approach can easily be adapted by organizations without the need for trained SAR experts. The subjective, manual image interpretation approach has proven useful in most regions due to the presence of both stabilized and non-stabilized landfast ice, but is subject to limitations outlined in *Section 4.*1.

5 Conclusion

In a time of rapidly changing ice conditions and continued interest in the Arctic by a range of stakeholders, we stress the need for new assessment strategies to support continued safe and efficient use of sea ice. InSAR is gaining growing attention in the sea ice scientific community and here we demonstrate its value for identifying and mapping newly defined classes of landfast ice while also highlighting the potentially substantial impact InSAR may have on the development of operational sea ice information products for both long-term strategic planning as well as short-term tactical decisions. Using interferograms generated by a standardized workflow, we show that multiple stability classes of landfast ice can be identified based on fringe density and continuity, which are indicative of differential ice motion occurring between SAR acquisitions. Along the Beaufort Sea coast of Alaska, we find that the landfast ice regime can be well described with three stability classes: bottomfast ice, where the sea ice is frozen to or resting on the seabed; stabilized ice, which is floating but anchored by islands or grounded ridges; and non-stabilized ice, which represent floating extensions seaward of any anchoring points. This finding was supported by comparison with the location of stable “nodes” identified through analysis of hundreds of landfast ice edge positions over the period 1996-2008 (Mahoney et al., 2014). Not only does this provide some validation of our results, but it demonstrates the ability of InSAR to capture in two snapshots what otherwise requires analysis of data over many years. With that said, the stability regimes in the Beaufort Sea and the Russian Arctic appear to be qualitatively different. This makes it challenging to directly adapt the proposed scheme to the East Siberian and Laptev Sea without including additional stability classes. This would allow for a more rigorous definition of landfast sea ice in different regions with implications for operational mapping.

The use of a standardized workflow facilitates large-scale application of this approach, which we demonstrated on a near-pan Arctic scale using 50 Sentinel-1 acquisition pairs during spring 2017. This allowed us to delineate the same classes of landfast ice in the Beaufort, Chukchi, East Siberian, Laptev, and Kara seas. It also enabled us to estimate and compare the total area covered by each stability class in each marginal sea. Bottomfast ice is found most extensively around river mouths and deltas and is most prevalent overall in the Laptev and the East Siberian seas, where it covers approximately 4.1×10^3 and 5.5×10^3 km^2, respectively. These two seas also contain the largest area of landfast ice with over 100×10^3 km^2 each. Even so, we found the largest amount of stabilized ice in the Beaufort Sea, where the overall ratio of stabilized to non-stabilized ice was the highest and close to unity. We found the Chukchi Sea to have the least area of stabilized ice and the highest proportion of non-stabilized ice. However, we note that these comparisons are based on the assumption that the landfast ice regimes in all these seas can be well described by the same three stability classes. Although we find evidence that other classes of landfast ice may exist in the Russian Arctic, our results clearly show that not all landfast ice is equally stable. Here, InSAR is potentially able to detect small-scale motions on scales reaching hundreds of km that have previously been overlooked.

We further demonstrate the scientific and operational value of InSAR over sea ice through the examination of interferograms of ice arches, which in this context can be considered as an additional stability class of quasi-landfast ice (e.g., "temporarily stabilized pack ice"). Preliminary analysis of the Nares Strait ice arch in 2017 suggests that interferograms may reveal early-warning signals of an imminent break-up. We also anticipate that inverse modeling of the interferograms of ice arches to estimate the small-scale strain field (Dammann et al., 2018b) may improve our ability to predict their formation. We also show how InSAR can provide valuable information for stakeholders enabling tracking of ice dynamics and stability on seasonal and year-to-year timescales. The ability to provide stability information to stakeholders also opens up for the development of operational guidelines in terms of what stability regimes should be prioritized or avoided.

This work builds on previous applications of InSAR to the study of landfast ice (Meyer et al., 2011;Berg et al., 2015;Dammert et al., 1998;Morris et al., 1999;Dammann et al., 2018b) and demonstrates what can be achieved over large areas with a standardized work flow. 2017 was the first year Sentinel-1 covered the Arctic coast with IW images necessary for this analysis. If this coverage continues, there will be considerable opportunity for development beyond what is presented here, including development of automated methods for delineating and classifying landfast ice suitable for incorporation into operational ice charts. Furthermore, through additional analysis of landfast ice and ice arches subject to different forcing conditions, we anticipate improving our understanding of stabilizing and destabilizing mechanisms, thereby allowing improved prediction of formation and break-up. This will not only enhance operational sea ice information available to stakeholders, but also allow us to better understand the response of coastal sea ice to a changing Arctic environment.

Acknowledgements

This work was funded by the Swedish National Space Agency (Dnr. 192/15). Sentinel-1 data are provided free of charge by the European Union Copernicus program. We acknowledge Alaska Satellite Facility for data access and in particular Bill Hauer for valuable data support.

Competing interests

The authors declare that they have no conflict of interest.

References

ACIA: Impacts of a Warming Arctic, Arctic Climate Impact Assessment, Cambridge University Press, Cambridge, UK, 144 pp., 2004.

Alexandrov, V. Y., Martin, T., Kolatschek, J., Eicken, H., Kreyscher, M., and Makshtas, A. P.: Sea ice circulation in the Laptev Sea and ice export to the Arctic Ocean: Results from satellite remote sensing and numerical modeling, Journal of Geophysical Research: Oceans, 105, 17143-17159, 2000.

Aporta, C., and Higgs, E.: Satellite culture - Global positioning systems, inuit wayfinding, and the need for a new account of technology, Curr Anthropol, 46, 729-753, 10.1086/432651, 2005.

Are, F., and Reimnitz, E.: An overview of the Lena River Delta setting: geology, tectonics, geomorphology, and hydrology, Journal of Coastal Research, 16, 1083-1093, 2000.

Bailey, W.: Oceanographic features of the Canadian Archipelago, Journal of the Fisheries Board of Canada, 14, 731-769, 1957.

Bamler, R., and Hartl, P.: Synthetic aperture radar interferometry, Inverse problems, 14, R1, 1998.

Barber, D., Babb, D., Ehn, J., Chan, W., Matthes, L., Dalman, L., Campbell, Y., Harasyn, M., Firoozy, N., and Theriault, N.: Increasing mobility of high Arctic sea ice increases marine hazards off the east coast of Newfoundland, Geophys Res Lett, 45, 2370-2379, 2018.

Bell, T., Briggs, R., Bachmayer, R., and Li, S.: Augmenting Inuit knowledge for safe sea-ice travel—The SmartICE information system, 2014 Oceans'14 St. John's, Newfoundland, 2014, 1-9, 2014.

Berg, A., Dammert, P., and Eriksson, L. E. B.: X-Band Interferometric SAR Observations of Baltic Fast Ice, IEEE Transactions on Geoscience and Remote Sensing, 53, 1248-1256, 10.1109/TGRS.2014.2336752, 2015.

Brothers, L. L., Hart, P. E., and Ruppel, C. D.: Minimum distribution of subsea ice-bearing permafrost on the US Beaufort Sea continental shelf, Geophys Res Lett, 39, 10.1029/2012GL052222 2012.

Comiso, J. C., and Hall, D. K.: Climate trends in the Arctic as observed from space, Wiley Interdisciplinary Reviews: Climate Change, 5, 389-409, 10.1002/wcc.277, 2014.

Dammann, D. O., Eicken, H., Meyer, F., and Mahoney, A.: Assessing small-scale deformation and stability of landfast sea ice on seasonal timescales through L-band SAR interferometry and inverse modeling, Remote Sens Environ, 187, 492-504, 10.1016/j.rse.2016.10.032, 2016.

Dammann, D. O.: Arctic sea ice trafficability - new strategies for a changing icescape, Ph.D. thesis, Department of Geosciences, University of Alaska Fairbanks, Fairbanks, Alaska, USA, 217 pp., 2017.

Dammann, D. O., Eicken, H., Saiet, E., Mahoney, A., Meyer, F., and George, J. C.: Traversing sea ice - linking surface roughness and ice trafficability through SAR polarimetry and interferometry IEEE Journal of Selected Topics in Applied Earth Observations and Remote Sensing, 11, 416-433, 10.1109/JSTARS.2017.2764961, 2017.

Dammann, D. O., Eicken, H., Mahoney, A., Meyer, F., and Betcher, S.: Assessing sea ice trafficability in a changing Arctic, Arctic, 71, 59-75, 10.14430/arctic4701, 2018a.

Dammann, D. O., Eicken, H., Mahoney, A., Meyer, F., Freymueller, J., and Kaufman, A. M.: Evaluating landfast sea ice stress and fracture in support of operations on sea ice using SAR interferometry, Cold Reg Sci Technol, 10.1016/j.coldregions.2018.02.001, 2018b.

Dammann, D. O., Eriksson, L. E. B., Mahoney, A., Stevens, C. W., Van der Sanden, J., Eicken, H., Meyer, F., and Tweedie, C.: Mapping Arctic bottomfast sea ice using SAR interferometry, Remote Sensing, 10(5), 720, 10.3390/rs10050720, 2018c.

Dammert, P. B. G., Lepparanta, M., and Askne, J.: SAR interferometry over Baltic Sea ice, Int J Remote Sens, 19, 3019-3037, 10.1080/014311698214163, 1998.

Dierking, W., Lang, O., and Busche, T.: Sea ice local surface topography from single-pass satellite InSAR measurements: a feasibility study, The Cryosphere, 11, 1967, 10.5194/tc-11-1967-2017, 2017.

Druckenmiller, M. L.: Alaska shorefast ice: interfacing geophysics with local sea ice knowledge and use, Ph.D. thesis, University of Alaska Fairbanks, Fairbanks, Alaska, 210 pp., 2011.

Druckenmiller, M. L., Eicken, H., George, J. C., and Brower, L.: Trails to the whale: reflections of change and choice on an Iñupiat icescape at Barrow, Alaska, Polar Geography, 36, 5-29, 10.1080/1088937X.2012.724459, 2013.

Eguíluz, V. M., Fernández-Gracia, J., Irigoien, X., and Duarte, C. M.: A quantitative assessment of Arctic shipping in 2010–2014, Scientific reports, 6, 30682, 2016.

Eicken, H., Dmitrenko, I., Tyshko, K., Darovskikh, A., Dierking, W., Blahak, U., Groves, J., and Kassens, H.: Zonation of the Laptev Sea landfast ice cover and its importance in a frozen estuary, Global and planetary change, 48, 55-83, 2005.

Eicken, H., Lovecraft, A. L., and Druckenmiller, M. L.: Sea-Ice System Services: A Framework to Help Identify and Meet Information Needs Relevant for Arctic Observing Networks, Arctic, 62, 119-136, 10.14430/arctic126, 2009.

Eicken, H., Jones, J., Meyer, F., Mahoney, A., Druckenmiller, M. L., Rohith, M., and Kambhamettu, C.: Environmental security in Arctic ice-covered seas: from strategy to tactics of hazard identification and emergency response, Mar Technol Soc J, 45, 37-48, doi.org/10.4031/MTSJ.45.3.1, 2011.

Eicken, H., and Mahoney, A. R.: Sea Ice: Hazards, Risks, and Implications for Disasters, in: Coastal and Marine Hazards, Risks, and Disasters, edited by: Ellis, J. T., Sherman, D. J., and Shroder, J. F., Elsevier Inc., Amsterdam, Netherlands, 381-399, 2015.

Ellis, B., and Brigham, L.: Arctic marine shipping assessment, Akureyri, Island, 2009.

Ferretti, A., Monti-Guarnieri, A., Prati, C., Rocca, F., and Massonet, D.: InSAR Principles-Guidelines for SAR Interferometry Processing and Interpretation, ESA Publications, TM-19, 2007.

Fienup-Riordan, A., and Rearden, A.: The ice is always changing: Yup'ik understandings of sea ice, past and present, in: SIKU: knowing Our Ice: Documenting Inuit Sea Ice knowledge and Use, edited by: Krupnik, I., Aporta, C., Gearheard, S., Laidler, G., and Holm, L. K., Springer, New York, 295-320, 2010.

Ford, J. D., Pearce, T., Gilligan, J., Smit, B., and Oakes, J.: Climate change and hazards associated with ice use in northern Canada, Arctic, Antarctic, and Alpine Research, 40, 647-659, 10.1657/1523-0430(07-040)[FORD]2.0.CO;2, 2008.

Giles, A. B., Massom, R. A., and Lytle, V. I.: Fast-ice distribution in East Antarctica during 1997 and 1999 determined using RADARSAT data, Journal of Geophysical Research: Oceans, 113, 10.1029/2007JC004139, 2008.

Hibler, W., Hutchings, J., and Ip, C.: Sea-ice arching and multiple flow states of Arctic pack ice, Annals of Glaciology, 44, 339-344, 2006.

Hirose, T., Kapfer, M., Bennett, J., Cott, P., Manson, G., and Solomon, S.: Bottomfast Ice Mapping and the Measurement of Ice Thickness on Tundra Lakes Using C-Band Synthetic Aperture Radar Remote Sensing, JAWRA Journal of the American Water Resources Association, 44, 285-292, 2008.

Hui, F., Zhao, T., Li, X., Shokr, M., Heil, P., Zhao, J., Zhang, L., and Cheng, X.: Satellite-Based Sea Ice Navigation for Prydz Bay, East Antarctica, Remote Sensing, 9, 518, 2017.

Johannessen, O. M., Alexandrov, V., Frolov, I. Y., Sandven, S., Pettersson, L. H., Bobylev, L. P., Kloster, K., Smirnov, V. G., Mironov, Y. U., and Babich, N. G.: Remote sensing of sea ice in the Northern Sea Route: studies and applications, Springer Science & Business Media, Chichester, United Kingdom, 2006.

Jones, J. M., Eicken, H., Mahoney, A. R., Rohith, M. V., Kambhamettu, C., Fukamachi, Y., Ohshima, K. I., and George, J. C.: Landfast sea ice breakouts: Stabilizing ice features, oceanic and atmospheric forcing at Barrow, Alaska, Continental Shelf Research, 126, 10.1016/j.csr.2016.07.015, 2016.

Krupnik, I., Aporta, C., Gearheard, S., Laidler, G. J., and Holm, L. K.: SIKU: knowing our ice, Springer, New York, 2010.

Kwok, R., Toudal Pedersen, L., Gudmandsen, P., and Pang, S.: Large sea ice outflow into the Nares Strait in 2007, Geophys Res Lett, 37, L03502, 10.1029/2009GL041872, 2010.

Li, S., Shapiro, L., McNutt, L., and Feffers, A.: Application of Satellite Radar Interferometry to the Detection of Sea Ice Deformation, Journal of the Remote Sensing Society of Japan, 16, 67-77, 1996.

Lovecraft, A. L., and Eicken, H.: North by 2020: perspectives on Alaska's changing social-ecological systems, University of Alaska Press, Fairbanks, Alaska, 2011.

Mahoney, A., Eicken, H., Graves, A., Shapiro, L., and Cotter, P.: Landfast sea ice extent and variability in the Alaskan Arctic derived from SAR imagery, Proceedings of the International Geoscience and Remote Sensing Symposium, Anchorage, AK, 2004, 2146-2149, 2004.

Mahoney, A., Eicken, H., Gaylord, A. G., and Shapiro, L.: Alaska landfast sea ice: Links with bathymetry and atmospheric circulation, Journal of Geophysical Research: Oceans, 112, 10.1029/2006JC003559, 2007a.

Mahoney, A., Eicken, H., and Shapiro, L.: How fast is landfast sea ice? A study of the attachment and detachment of nearshore ice at Barrow, Alaska, Cold Reg Sci Technol, 47, 233-255, 10.1016/J.Coldregions.2006.09.005, 2007b.

Mahoney, A., Eicken, H., Gaylord, A. G., and Gens, R.: Landfast sea ice extent in the Chukchi and Beaufort Seas: The annual cycle and decadal variability, Cold Reg Sci Technol, 103, 41-56, 10.1016/J.Coldregions.2014.03.003, 2014.

Marbouti, M., Praks, J., Antropov, O., Rinne, E., and Leppäranta, M.: A Study of Landfast Ice with Sentinel-1 Repeat-Pass Interferometry over the Baltic Sea, Remote Sensing, 9, 833, 10.3390/rs9080833, 2017.

Meier, W. N., Hovelsrud, G. K., Oort, B. E., Key, J. R., Kovacs, K. M., Michel, C., Haas, C., Granskog, M. A., Gerland, S., and Perovich, D. K.: Arctic sea ice in transformation: A review of recent observed changes and impacts on biology and human activity, Reviews of Geophysics, 52, 185-217, 2014.

Meyer, F. J., Mahoney, A. R., Eicken, H., Denny, C. L., Druckenmiller, H. C., and Hendricks, S.: Mapping arctic landfast ice extent using L-band synthetic aperture radar interferometry, Remote Sens Environ, 115, 3029-3043, 10.1016/J.Rse.2011.06.006, 2011.

Meyer, F. J., McAlpin, D., Gong, W., Ajadi, O., Arko, S., Webley, P., and Dehn, J.: Integrating SAR and derived products into operational volcano monitoring and decision support systems, ISPRS Journal of Photogrammetry and Remote Sensing, 100, 106-117, 2015.

Morris, K., Li, S., and Jeffries, M.: Meso-and microscale sea-ice motion in the East Siberian Sea as determined from ERS-I SAR data, Journal of Glaciology, 45, 370-383, 1999.

Muckenhuber, S., and Sandven, S.: Open-source sea ice drift algorithm for Sentinel-1 SAR imagery using a combination of feature tracking and pattern matching, The Cryosphere, 11, 1835, 2017.

Orviku, K., Jaagus, J., and Tõnisson, H.: Sea ice shaping the shores, Journal of Coastal Research, 681, 2011.

Potter, R., Walden, J., and Haspel, R.: Design and construction of sea ice roads in the Alaskan Beaufort Sea, Offshore Technology Conference, Houston, Texas, 1981

Reimnitz, E., Dethleff, D., and Nürnberg, D.: Contrasts in Arctic shelf sea-ice regimes and some implications: Beaufort Sea versus Laptev Sea, Marine Geology, 119, 215-225, 1994.

Screen, J. A., and Simmonds, I.: The central role of diminishing sea ice in recent Arctic temperature amplification, Nature, 464, 1334-1337, 2010.

Selyuzhenok, V., Krumpen, T., Mahoney, A., Janout, M., and Gerdes, R.: Seasonal and interannual variability of fast ice extent in the southeastern Laptev Sea between 1999 and 2013, Journal of Geophysical Research: Oceans, 120, 7791-7806, 10.1002/2015JC011135, 2015.

Selyuzhenok, V., Mahoney, A., Krumpen, T., Castellani, G., and Gerdes, R.: Mechanisms of fast-ice development in the south-eastern Laptev Sea: a case study for winter of 2007/08 and 2009/10, Polar Research, 36, 1411140, 2017.

Smith, T. G.: Polar bear predation of ringed and bearded seals in the land-fast sea ice habitat, Canadian Journal of Zoology, 58, 2201-2209, 1980.

Solomon, S. M., Taylor, A. E., and Stevens, C. W.: Nearshore ground temperatures, seasonal ice bonding, and permafrost formation within the bottom-fast ice zone, Mackenzie Delta, NWT, Proceedings of the Ninth International Conference on Permafrost, University of Alaska Fairbanks, Fairbanks, Alaska, 2008, 1675-1680, 2008.

Stephenson, S. R., Smith, L. C., and Agnew, J. A.: Divergent long-term trajectories of human access to the Arctic, Nat Clim Change, 1, 156-160, 10.1038/Nclimate1120, 2011.

Stevens, C. W., Moorman, B. J., and Solomon, S. M.: Detection of frozen and unfrozen interfaces with ground penetrating radar in the nearshore zone of the Mackenzie Delta, Canada, Proceedings of the Ninth International Conference on Permafrost, University of Alaska Fairbanks, Fairbanks, Alaska, 2008, 1711-1716, 2008.

Stevens, C. W., Moorman, B. J., and Solomon, S. M.: Interannual changes in seasonal ground freezing and near-surface heat flow beneath bottom-fast ice in the near-shore zone, Mackenzie Delta, NWT, Canada, Permafrost and Periglacial Processes, 21, 256-270, 2010.

Stevens, C. W.: Controls on Seasonal Ground Freezing and Permafrost in the Near-shore Zone of the Mackenzie Delta, NWT, Canada, University of Calgary, 2011.

Stroeve, J. C., Serreze, M. C., Holland, M. M., Kay, J. E., Malanik, J., and Barrett, A. P.: The Arctic's rapidly shrinking sea ice cover: a research synthesis, Climatic Change, 110, 1005-1027, 10.1007/S10584-011-0101-1, 2012.

Thomas, D. N.: Sea ice, John Wiley & Sons, Chichester, United Kingdom, 2017.

Vincent, F., Raucoules, D., Degroeve, T., Edwards, G., and Abolfazl Mostafavi, M.: Detection of river/sea ice deformation using satellite interferometry: limits and potential, Int J Remote Sens, 25, 3555-3571, 2004.

Werner, C., Wegmüller, U., Strozzi, T., and Wiesmann, A.: Gamma SAR and interferometric processing software, Proceedings of the ERS-ENVISAT symposium, Gothenburg, Sweden, 2000, 1620

Wilson, K. J., Falkingham, J., Melling, H., and De Abreu, R.: Shipping in the Canadian Arctic: other possible climate change scenarios, Proceedings of the International Geoscience and Remote Sensing Symposium, Anchorage, AK, 2004, 1853-1856, 2004.

Yu, Y., Stern, H., Fowler, C., Fetterer, F., and Maslanik, J.: Interannual Variability of Arctic Landfast Ice between 1976 and 2007, J Climate, 27, 227-243, 10.1175/JCLI-D-13-00178.1, 2014.

The Cryosphere Discuss., https://doi.org/10.5194/tc-2018-129
Manuscript under review for journal The Cryosphere
Discussion started: 11 July 2018

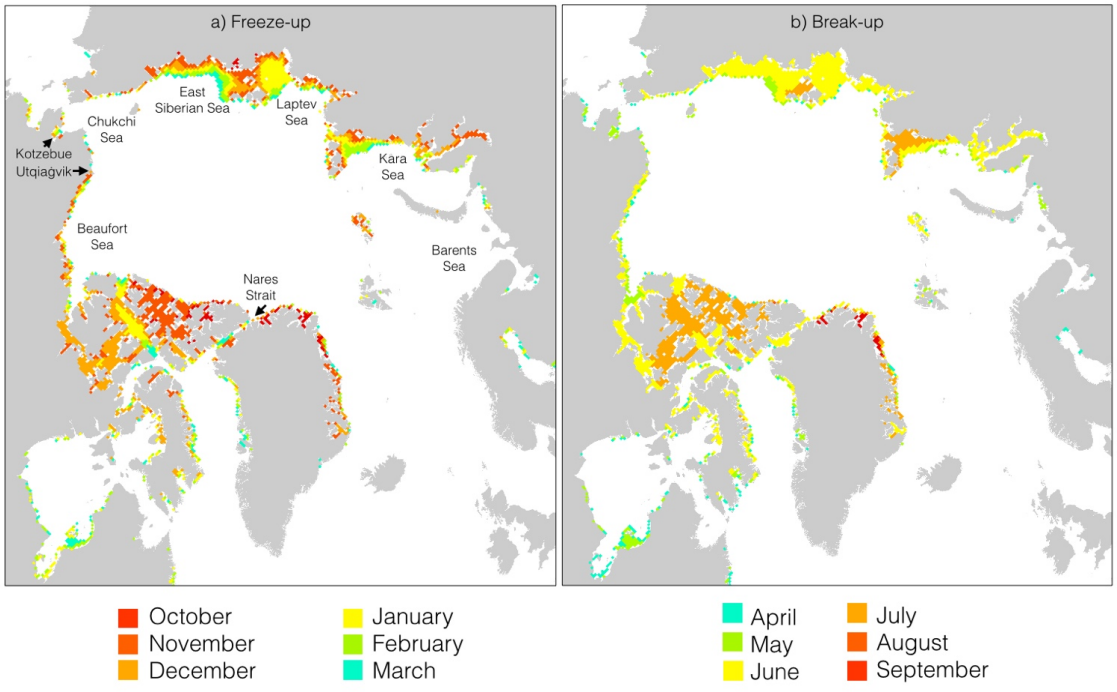

Figure 1: (a) Oct - Mar (Freeze-up) and (b) Apr - Sep (break-up) monthly mean landfast sea ice extent (1976 - 2007) derived from ice sea ice charts based on optical instruments and SAR. The data for this figure was obtained from the National Snow and Ice Data Center (Yu et al., 2014).

The Cryosphere Discuss., https://doi.org/10.5194/tc-2018-129
Manuscript under review for journal The Cryosphere
Discussion started: 11 July 2018

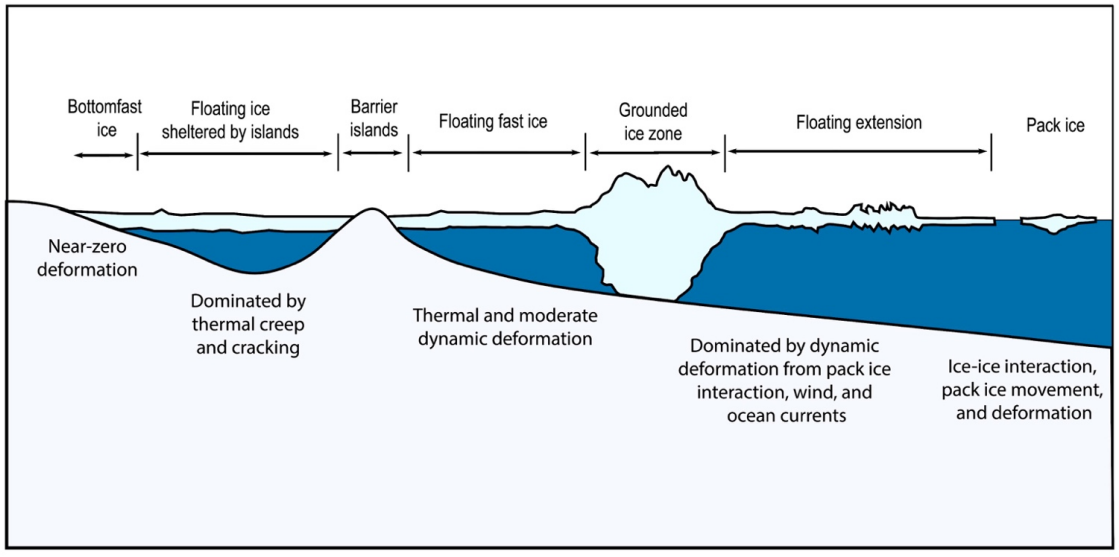

Figure 2: Example of landfast sea ice where different regimes possess different levels of stability.

The Cryosphere Discuss., https://doi.org/10.5194/tc-2018-129
Manuscript under review for journal The Cryosphere
Discussion started: 11 July 2018

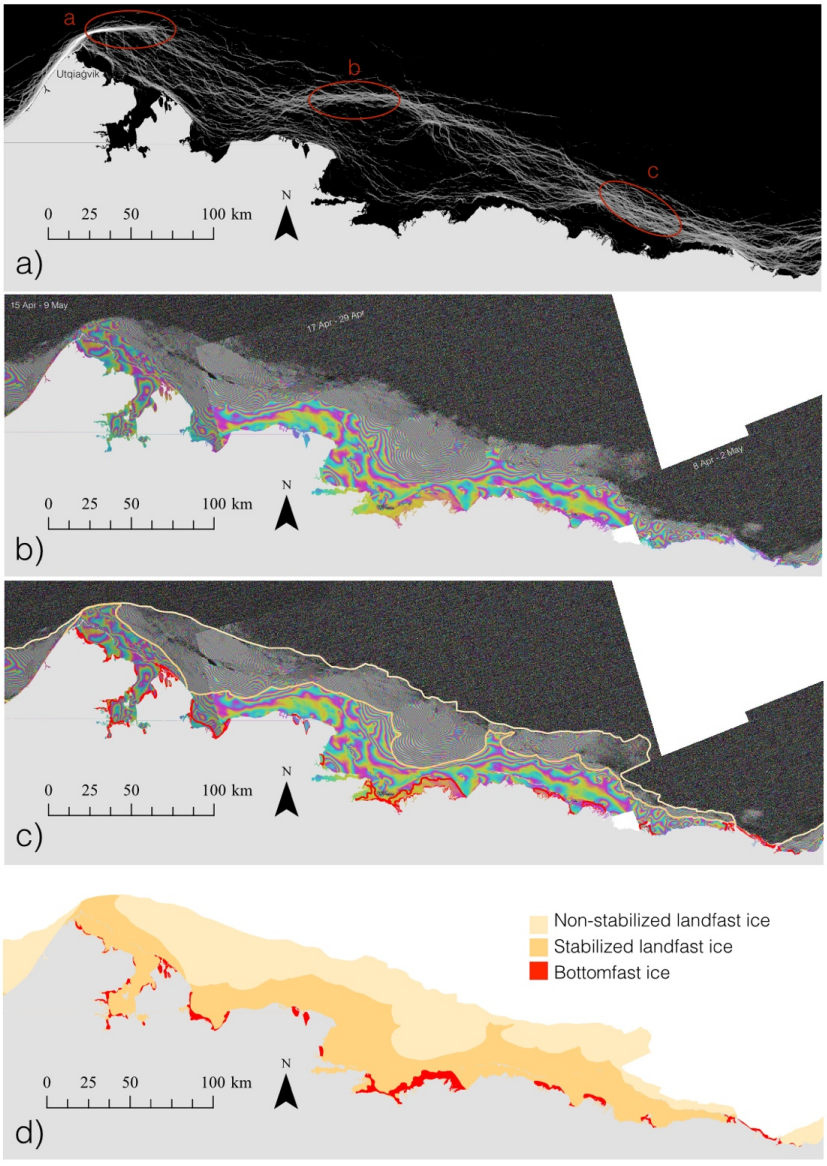

Figure 3: (a) Landfast ice edge occurrence delineated for the period 1996–2008 over the Alaska Beaufort Sea (Mahoney et al. 2014), (b) Sentinel-1 interferograms of landfast ice between mid April and mid May 2017 (c) delineation of landfast ice, grounded landfast ice, and bottomfast ice superimposed on the interferograms, (d) different landfast ice regimes derived from the interferograms.

The Cryosphere Discuss., https://doi.org/10.5194/tc-2018-129
Manuscript under review for journal The Cryosphere
Discussion started: 11 July 2018

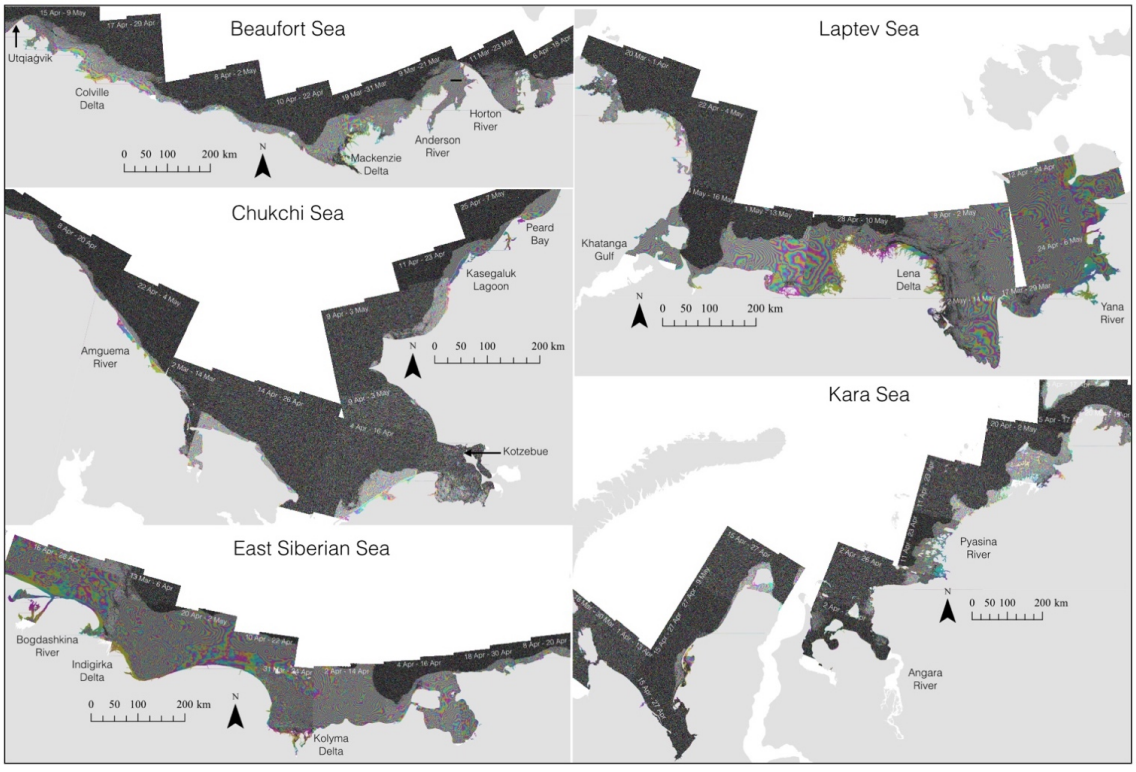

Figure 4: 50 Sentinel-1 interferograms derived from image pairs acquired between March and May, 2017.

5

The Cryosphere Discuss., https://doi.org/10.5194/tc-2018-129
Manuscript under review for journal The Cryosphere
Discussion started: 11 July 2018

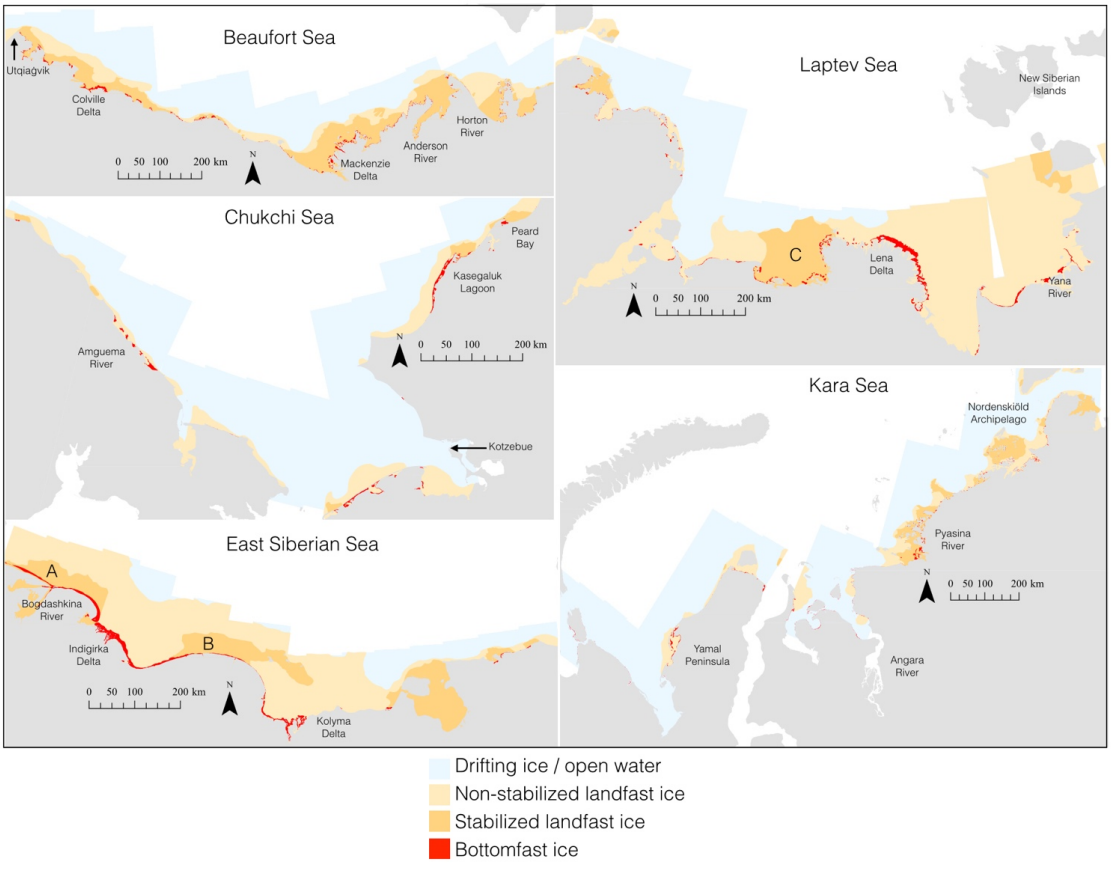

Figure 5: InSAR-derived delineation of non-stabilize and stabilized landfast ice and bottomfast ice from 50 Sentinel-1 image pairs acquired between March and May, 2017.

The Cryosphere Discuss., https://doi.org/10.5194/tc-2018-129
Manuscript under review for journal The Cryosphere
Discussion started: 11 July 2018

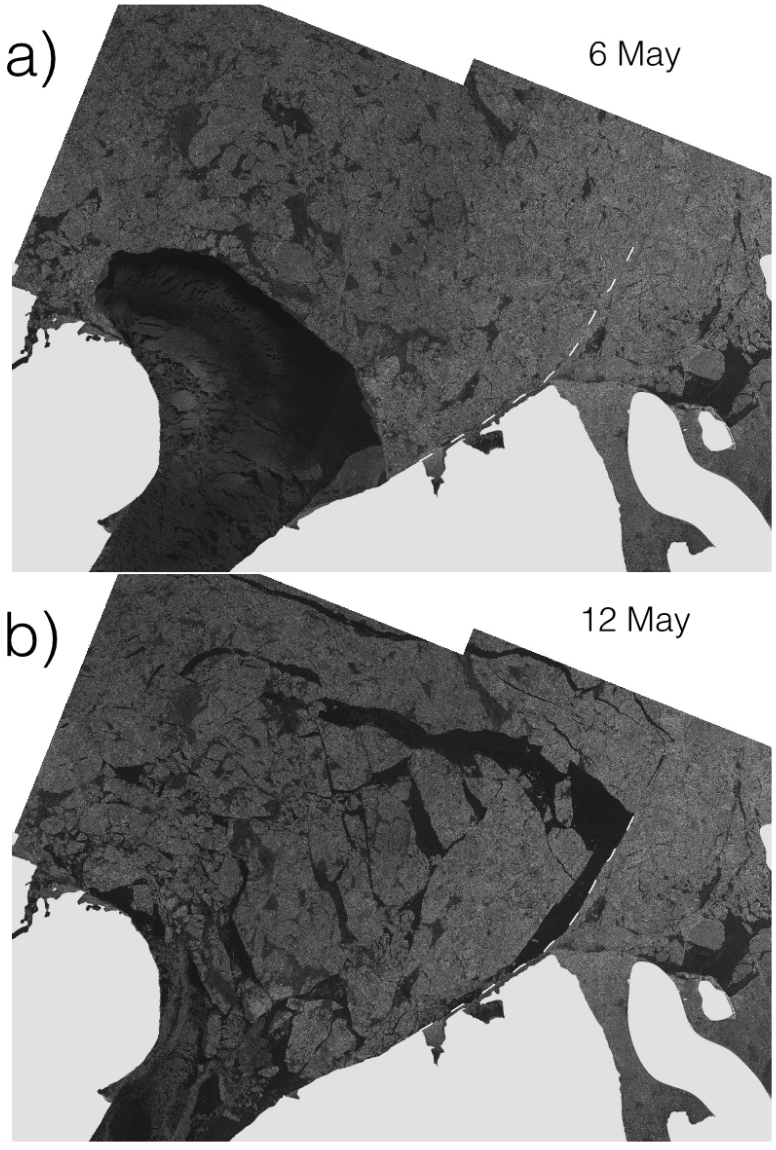

Figure 6: Backscatter images over an ice arch in Nares Strait during 2017 before (a) and after (b) failure. The dashed line represents the line of failure. Land is masked out in light gray.

The Cryosphere Discuss., https://doi.org/10.5194/tc-2018-129
Manuscript under review for journal The Cryosphere
Discussion started: 11 July 2018

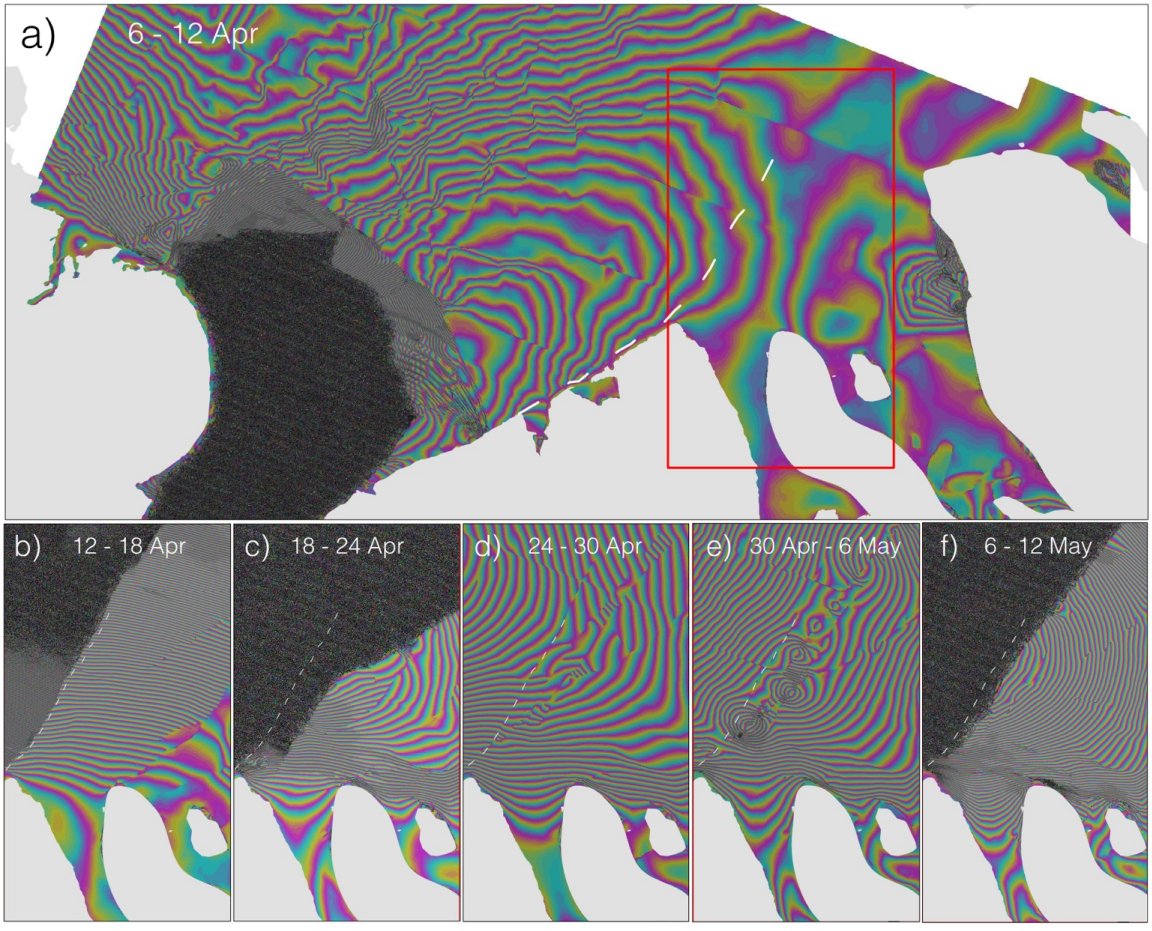

Figure 7: Interferogram over the Nares Strait ice arch in 2017 covering the time period 6 - 12 Apr. (a). Smaller panels show consecutive interferograms within the box for 12 - 18 Apr (b), 18 - 24 Apr (c), 24 - 30 Apr (d), 30 Apr - 6 May (e), and 6 - 12 May (f). The dashed line represents the line separating the fast and moving ice in Figure 6b. Land is masked out in light gray.

The Cryosphere Discuss., https://doi.org/10.5194/tc-2018-129
Manuscript under review for journal The Cryosphere
Discussion started: 11 July 2018

Table 1: Landfast sea ice regimes categorized according to stability

	Landfast ice regime	Stability
1	Bottomfast sea ice (i.e., ice frozen to or in broad contact with the sea floor)	Completely stable. Ice is frozen to or resting on the sea floor restricting lateral motion. Vertical tide jacking may occur and subsides as the ice thickens.
2	Floating ice sheltered in lagoons or fjords	High stability. Ice is largely enclosed by land and is sheltered from more dynamic ice. Deformation is dominated by cm- to dm-scale thermal creep and fracture.
3	Floating ice sheltered by grounded ridges or islands	Moderate stability. Ice is supported by point features largely inhibiting break out events. In addition to thermal creep, internal stress from more dynamic ice can propagate in between pinning points resulting in dm- to m-scale non-elastic deformation.
4	Floating ice extensions	Low stability. Dominated by m-scale deformation from ice, wind, and ocean forcing. Persistent inelastic deformation can lead to accumulated strain on the order of tens of meters on time-scales exceeding several weeks. The ice may remain attached (Mahoney et al., 2004) or can break-off from the stabilized ice.

5

The Cryosphere Discuss., https://doi.org/10.5194/tc-2018-129
Manuscript under review for journal The Cryosphere
Discussion started: 11 July 2018

Table 2: Stability regimes identified using InSAR and typical deformation rates

	Stability regime	Identified by	Deformation rate (cm/km/month)
1	Bottomfast ice	No identifiable phase difference from the adjacent land	0
2	Stabilized ice	Poorly defined, widely spaced fringes or abruptly reduced fringe spacing compared to offshore ice	~0.1 – ~1
3	Non-stabilized ice	Tightly spaced, well defined fringes	< ~100

The Cryosphere Discuss., https://doi.org/10.5194/tc-2018-129
Manuscript under review for journal The Cryosphere
Discussion started: 11 July 2018

Table 3: Approximate area coverage of landfast ice regimes (in thousand km^2).

Area	Bottomfast ice	Stabilized	Non-stabilized	Total area of landfast ice	Non-stabilized / stabilized
Beaufort Sea	2.5	37	38	77	1.0
Chukchi Sea	1.8	2.7	54	58	20
East Siberian Sea	5.5	25	118	148	4.7
Laptev Sea	4.1	27	184	215	6.8
Kara Sea	2.5	18	38	58	2.1